

[Click here to view linked References](#)

1

Title: Protective properties of grape-seed proanthocyanidins in human ex vivo acute colonic dysfunction induced by dextran sodium sulphate.

Authors: Carlos González-Quilen¹, Carme Grau-Bové¹, Rosa Jorba-Martín², Aleidis Caro-Tarragó², Montserrat Pinent¹, Anna Ardévol¹, Raúl Beltrán-Debón¹, Ximena Terra^{1,*}, M Teresa Blay^{1,*}.

Affiliation:

¹Universitat Rovira i Virgili, Departament de Bioquímica i Biotecnologia, MoBioFood Research Group, 43007 Tarragona, Spain.

²Servei de Cirurgia General i de l'Aparell Digestiu, Hospital Universitari Joan XXIII, Tarragona, Spain.

*Both authors contributed equally to this work

Correspondence: Raúl Beltrán-Debón; raul.beltran@urv.cat; Tel.: +34-977-55- 8778.

Characters: 42,541

Abstract

Purpose: Anti-inflammatory and barrier protective properties have been attributed to proanthocyanidins in the context of intestinal dysfunction, however little information is available about the impact of these phytochemicals on intestinal barrier integrity and immune response in the human. Here we assessed the putative protective properties of a grape-seed proanthocyanidin extract (GSPE) against dextran sodium sulphate (DSS)-induced acute dysfunction of the human colon in an Ussing chamber system.

Methods: Human proximal and distal colon tissues from colectomized patients were submitted ex vivo to a 30-minute preventive GSPE treatment (50 or 200 $\mu\text{g mL}^{-1}$) followed by 1-hour incubation with DSS (12% w v⁻¹). Transepithelial electrical resistance (TEER), permeation of a fluorescently-labelled dextran (FD4) and proinflammatory cytokine release (tumor necrosis factor (TNF)- α and interleukin (IL)-1 β) of colonic tissues were determined.

Results: DSS reduced TEER (45-52%) in both the proximal and distal colon; however, significant increments in FD4 permeation (4-fold) and TNF- α release (61%) were observed only in the proximal colon. The preventive GSPE treatment decreased DSS-induced TEER loss (20-32%), FD4 permeation (66-73%) and TNF- α release (22-33%) of the proximal colon dose-dependently. The distal colon was not responsive to the preventive treatment but showed a reduction in IL-1 β release below basal levels with the highest GSPE concentration.

Conclusions: Our results demonstrate potential preventive effects of GSPE on human colon dysfunction. Further studies are required to test whether administering GSPE could be a complementary therapeutic approach in colonic dysfunction associated with metabolic disorders and inflammatory bowel disease.

Keywords: Human colon, Ussing chamber, inflammation, permeability, flavonoid, procyanidin

1. Introduction

Intestinal dysfunction, characterized by an increase in epithelial permeability and mucosal inflammation, is a manifestation commonly observed in obesity and inflammatory bowel disease (ulcerative colitis and Crohn's disease; IBD) [1]. Intestinal barrier integrity is a key feature in human health as it is essential for maintaining normal intestinal permeability. When the barrier function is compromised by detrimental agents (e.g. diet components and chemicals) the permeability is altered, which can lead to the translocation and dissemination of luminal content into the underlying tissue, including bacterial lipopolysaccharides (LPS) [1, 2]. Chronic exposition to these elements triggers the ubiquitous expression of inflammatory transcription factors, such as nuclear factor kappa-light-chain-enhancer of activated B cells (NF- κ B), which leads to the production of proinflammatory cytokines like tumor necrosis factor (TNF)- α , interleukin (IL)-1 β and IL-6, with a concomitant decrease in the anti-inflammatory cytokines and proteins [3, 4]. This disruption of the intestinal epithelial-cell barrier is closely associated with the onset of metabolic disorders [1, 5, 6].

The link between alterations of the intestinal barrier function and inflammation has been studied in animals exposed to various chemicals [7]. In recent years, many in vivo experiments have employed dextran sodium sulphate (DSS) as a chemical inductor of colonic dysfunction because of its simplicity and reproducible effect that closely resembles human ulcerative colitis [8]. DSS is a water-soluble sulphated polysaccharide of negative charge and highly variable molecular weight. The administration in murines of 40-50 kDa DSS added to drinking water (up to 10% w v⁻¹) results in the erosion of the colon epithelium, which compromises barrier integrity and increases colonic epithelial permeability [8]. The DSS-induced damage is almost completely restricted to the colon mucosa, although the reason for this is not known. It has been suggested that DSS forms nano-lipocomplexes with medium-chain-length fatty acids in the colon, which disrupts the epithelial barrier [9].

26 Interventions for improving intestinal barrier integrity have shown promising results in the
27 context of inflammatory bowel disease and metabolic disorders [1]. Multiple studies using
28 experimental animals demonstrate the beneficial effects of proanthocyanidin, which can
29 ameliorate intestinal dysfunction derived from the diet [10, 11], spontaneously-induced or
30 produced by chemical agents [12]. Proanthocyanidins are oligomeric and polymeric flavan-3-ols,
31 mainly composed of (+)-catechin and (-)-epicatechin monomers. They are present in a wide
32 variety of plant derived foods and beverages and constitute one of the most abundant groups of
33 phenolic compounds in the human diet [13]. Proanthocyanidins from grape seeds have been
34 shown to improve colonic permeability alterations and local inflammation induced by DSS and
35 other chemicals in experimental rats, often exerting an effect comparable to sulfasalazine, an anti-
36 inflammatory drug [14–16]. The metabolic effects of grape-seed proanthocyanidins on intestinal
37 mucosa described in these in vivo studies include increasing antioxidant enzyme activity and
38 reducing proinflammatory mediators, such as TNF- α and IL-1 β , as well as the associated immune
39 cell infiltration. It has been proposed that the reduction in mucosal inflammation is mediated by
40 the inhibition of the NF- κ B signal transduction pathway [17, 18].

41 Although there is much evidence supporting the gut-protective properties of grape-seed
42 proanthocyanidins, there are few studies that analyze the efficacy of these phytochemicals in
43 humans and thus efforts should focus on this. The Ussing chamber technique is a valuable tool
44 for studying human intestinal function [19, 20]. The set-up consists of two half chambers
45 separating the apical and basolateral domains of the mucosal preparation, thus mimicking the in
46 vivo situation of the epithelium and permitting an accurate prediction of intestinal function. In
47 this set-up, tissue integrity can be monitored by electrophysiological parameters such as the
48 transepithelial electrical resistance (TEER), that reflects the ionic conductance of the paracellular
49 pathway. Furthermore, preserving the tissue architecture maintains the interplay between the
50 different cell types, which not only makes it possible to study site-specific transport of molecules

51 across the epithelium but also the metabolic effects of bioactives administered in a donor
52 compartment that simulates the intestinal lumen [19].

53 In the present study, healthy/normal colon tissues from donor oncology patients who
54 underwent colectomy were used to perform Ussing chamber-based experiments. In these ex vivo
55 assays, human proximal and distal colon tissues were exposed to DSS as an inductor of acute
56 dysfunction to evaluate the putative barrier-protective and anti-inflammatory properties of a
57 grape-seed proanthocyanidin extract (GSPE).

58 **2. Materials and methods**

59 *Proanthocyanidin extract*

60 The grape-seed proanthocyanidin extract (GSPE) was provided by Les Dérivés Résiniques
61 et Terpéniques (batch number 124029; Dax, France). According to the manufacturer the GSPE has
62 the following composition: monomers of flavan-3-ols (21.3%), dimers (17.4%), trimers (16.3%),
63 tetramers (13.3%) and oligomers (5–13 units; 31.7%) of proanthocyanidins. A detailed analysis of
64 the monomeric, dimeric, and trimeric structures of the GSPE can be found in the work by
65 Margalef et al. [21]. The GSPE was dissolved in DMSO 50% to prepare a stock solution of
66 100 mg mL⁻¹.

67 *Collection of human tissues*

68 Human colon tissues were collected from 62 consecutive donor patients with pathologically
69 confirmed colorectal carcinoma and a median age of 65 years (range: 28–82 years), who
70 underwent colon surgery between 2016 and 2019 in the University Hospital Joan XXIII
71 (Tarragona, Spain). Exclusion criteria included the consumption of anti-inflammatory drugs,
72 alcohol abuse and the presence of IBD or celiac disease as these would alter intestinal functioning.
73 All donor patients gave informed consent and the study was approved by the ethics committee
74 of the University Hospital Joan XXIII (ref. CEIm 101/2017). The characteristics of patients included

75 in this study are summarized in Table 1. Non-diseased tissues that were not strictly needed for
76 diagnosis purposes were excised from the proximal colon (cecum, ascending, hepatic flexure, and
77 transverse colon; n=27) and distal colon (splenic flexure, descending and sigmoid colon; n=34).
78 After resection, these colon tissues were transferred from the hospital within 30 min in ice-cold
79 Krebs-Ringer bicarbonate (KRB) buffer (pH 7.4) saturated with 95% oxygen and 5% CO₂. After
80 rinsing, tissues were mounted in a plastic tube to facilitate the removal of the serosal and outer
81 muscular layers with a scalpel (stripping). The stripped preparations were placed apical side up
82 on Parafilm M (Heathrow Scientific, Vernon Hills, IL, USA) and segments of approximately
83 1.5 × 1.0 cm were cut for the Ussing chamber experiments.

84 *Ussing chamber experiments*

85 Depending on tissue availability, up to four stripped proximal or distal colon segments of
86 one patient were placed in 0.237 cm² aperture Ussing chambers (Dipl.-Ing. Mussler Scientific
87 Instruments, Aachen, Germany) for each experiment. Ussing chambers were bathed apically and
88 basolaterally with 1.5 mL of fresh KRB buffer (pH 7.4). The basolateral bathing solutions
89 contained 10 mM of glucose (Panreac, Barcelona, Spain) and were osmotically balanced in the
90 apical compartments with 10 mM of mannitol (Sigma, Madrid, Spain). Bathing solutions were
91 continuously bubbled with a O₂/CO₂ (95%/5%) gas mixture and circulated in water-jacketed
92 reservoirs kept at 37 °C.

93 After a 20-30-min equilibration period, the colon segments were randomly assigned to one
94 of four experimental conditions (Fig. 1). The bathing solution of the apical compartments was
95 replaced by KRB buffer containing GSPE at 50 µg mL⁻¹ (GSPE50-DSS condition) or 200 µg mL⁻¹
96 (GSPE200-DSS condition) or plain KRB buffer (DSS condition). The DMSO concentration was
97 kept at ≤ 0.1% in the apical media. A KRB buffer with protease inhibitors (10 µM amastatin (Enzo
98 Life Sciences, Madrid, Spain), 500 KIU aprotinin (Sigma, Madrid, Spain) and 0.1% bovine serum
99 albumin fatty acid free) was added to the basolateral compartments. Tissues were incubated for

100 30 min, after which the apical media were replaced by KRB buffer containing 12% w v⁻¹ of dextran
101 sodium sulphate (DSS, MW: 36,000–50,000; MP Biomedicals, Solon, OH, USA). After one
102 additional hour, the basolateral media were stored at –80 °C for further analysis. A control (Ctrl
103 condition) with plain KRB buffer was also included to assess the effect of the DSS.

104 *Histology*

105 Stripped and non-stripped colon segments were haematoxylin-eosin stained to evaluate the
106 tissue structure after stripping. Tissues were fixed in 4% diluted formaldehyde. After 24 h of
107 fixation, the tissues were successively dehydrated (alcohol/ethanol 70%, 96% and 100%; plus
108 xylol/dimethylbenzene) and paraffin infiltration-immersed at 52 °C. Then, sections 2 µm thick
109 (Microm HM 355S, Thermo Scientific) were obtained, deposited on slides (JP Selecta Paraffin
110 Bath), and subjected to automated hematoxylin-eosin staining (Shandon Varistain Gemini,
111 Thermo Scientific).

112 *Electrophysiological parameters*

113 A four-electrode system coupled to an external 6-channel voltage/current clamp electronic
114 unit (Dipl.-Ing. Mussler Scientific Instruments, Aachen, Germany) was used for monitoring the
115 electrophysiological parameters in each Ussing chamber. One pair of Ag/Cl electrodes was used
116 for measuring the potential difference (PD) and another pair for the current passage. The
117 spontaneous transepithelial PD was measured under open-circuit conditions after appropriate
118 correction for fluid resistance. TEER (ohm cm²) was calculated every 30 minutes from the
119 transepithelial PD and the short-circuit current in accordance with Ohm's law.

120 *Paracellular transport of fluorescently labeled dextran*

121 A stock solution of 110 mg mL⁻¹ of 4-kDa fluorescein isothiocyanate-dextran (FD4; TdB
122 Consultancy AB, Uppsala, Sweden) was prepared in phosphate-buffered saline. FD4 was added
123 apically in each Ussing chamber at a final concentration of 5.6 mg mL⁻¹ and incubated for 1 h

124 during the induction of acute colonic dysfunction by DSS. The amount of FD4 that crossed to the
125 basolateral compartment was measured in a PerkinElmer LS-30 fluorimeter (Beaconsfield, U.K.)
126 at $\lambda_{exc}=430$ nm and $\lambda_{em}=540$ nm and compared with a FD4 standard curve. FD4 transport across
127 the colon mucosa was calculated as apparent permeability (P_{app}) using the following equation:

$$128 \quad P_{app} \text{ (mL/cm}^2 \times \text{s)} = (V/A \times t) \times (C_{ba}/C_{ap}),$$

129 where V is the basolateral volume, A is the exposed surface area, t is the incubation time and C_{ba}
130 and C_{ap} are the concentrations of FD4 in the basolateral and apical media, respectively. To
131 compare the permeation of FD4 between the DSS and GSPE-DSS experimental conditions, values
132 were taken relative to the Ctrl levels.

133 *Proinflammatory cytokine release*

134 Human TNF- α and IL-1 β levels were determined using commercially available ELISA kits
135 according to the manufacturer's instructions (Thermo Fisher Scientific, Waltham, MA, USA).
136 Cytokine levels corresponded to the total amount released from colon tissues to the basolateral
137 media of each Ussing chamber at the end of the experiments. The absorbances were measured
138 with a BioTek Eon microplate spectrophotometer (BioTek Instruments Inc., Winooski, VT, USA)
139 at 450 nm and cytokine levels were expressed as picograms per milliliter. The analytical
140 sensitivities of the assays were 0.13 and 0.3 pg mL⁻¹, respectively.

141 *Statistical analysis*

142 Unless otherwise indicated, results are expressed as the mean \pm standard error of the mean
143 (SEM). The mean represents the average value of determinations performed in n patients. The
144 sample size (n) for each variable measured is indicated in the corresponding figure caption.
145 Descriptive statistics and comparisons between groups were assessed with unpaired one-sided
146 Student's t -tests, and P -values <0.05 were considered statistically significant. Analyses were

147 performed with the XLSTAT 2019.1.3 software (Addinsoft, NY, USA). Linear regressions were
148 fitted in Microsoft Excel 2016 software (Microsoft Corporation, Redmond, WA, USA).

149 **3. Results**

150 *Structural evaluation of colonic tissues after removal of the external muscular layer*

151 We evaluated the protective properties of the GSPE in the human colon in DSS-induced
152 dysfunctional mucosa. For this purpose, we mounted stripped preparations from human
153 proximal and distal colon tissues in an Ussing chamber system. The stripped preparations were
154 structurally conserved and consisted of the epithelial cell layer, the lamina propria, the
155 muscularis mucosae and the submucosal layer (Fig. 2b).

156 *Electrophysiological parameters of colonic tissues*

157 The basal electrophysiological parameters of all colon segments were measured. The
158 spontaneous transepithelial PD and initial TEER values were -0.66 ± 0.13 mV and
159 41.6 ± 1.7 ohm cm^2 for the proximal colon ($n=27$) and -0.42 ± 0.13 mV and 31.8 ± 1.4 ohm cm^2 ($n=34$)
160 for the distal colon. TEER differences between the proximal and distal colon were statistically
161 significant ($P < 0.01$). Barrier integrity is malleable and depends on multiple factors. Therefore,
162 potential differences in the initial TEER due to gender were evaluated in the proximal colon
163 (males ($n=17$): 39.6 ± 2.0 ohm cm^2 vs. females ($n=10$): 45.0 ± 3.1 ohm cm^2 ; $P > 0.05$) and distal colon
164 (males ($n=21$): 32.5 ± 1.7 ohm cm^2 vs. females ($n=13$): 30.7 ± 2.2 ohm cm^2 ; $P > 0.05$). We also performed
165 correlations between BMI, age and initial TEER values in order to discard a potential influence of
166 the patient's body weight and/or age on differences in the inter-variability of tissue integrity (Fig.
167 3). There were no statistically significant correlations between these variables in any colon region.
168 TEER values of the control conditions did not show significant changes during the 90-minute
169 experiments in either kind of tissue (Fig. 4a).

170 *Basal macromolecular permeability of the proximal and distal colon*

171 We found detectable FD4 permeations in the control conditions of the proximal ($6.3 \pm 1.4 \times 10^{-6}$
172 $\text{mL cm}^{-2} \text{s}^{-1}$, $n=15$) and distal colon ($2.5 \pm 0.5 \times 10^{-6} \text{ mL cm}^{-2} \text{s}^{-1}$, $n=15$) at the end of the experiments.
173 Differences were statistically significant ($P < 0.05$) and in agreement with those found in TEER.

174 *A preventive GSPE treatment attenuates DSS-induced permeability in the proximal colon.*

175 The presence of DSS had a detrimental effect on tissue integrity. This effect was more severe
176 in the proximal colon with a 44% reduction in TEER at 90 min compared to the control ($P < 0.01$;
177 Fig. 4a). In the distal colon a reduction of 37% at 90 min was estimated ($P < 0.01$). The loss of tissue
178 integrity induced by DSS came with a 2-4-fold increase in FD4 permeation to the basolateral
179 media. However, the effect of DSS on FD4 permeation was only statistically significant in the
180 proximal colon (DSS: $8.8 \pm 2.5 \times 10^{-6} \text{ mL cm}^{-2} \text{s}^{-1}$, $n=15$ vs. Ctrl: $2.5 \pm 0.5 \times 10^{-6} \text{ mL cm}^{-2} \text{s}^{-1}$, $n=16$; $P < 0.05$).

181 Even though the presence of the GSPE in the apical medium did not significantly change the
182 TEER of the proximal or distal colon during the initial 30-minute incubation at any concentration
183 ($P > 0.05$; Fig. 4a), interestingly GSPE attenuated the DSS-induced decreased integrity in the
184 proximal colon at 60 and 90 min ($P < 0.05$). This effect was dose dependent and therefore more
185 pronounced in the GSPE200-DSS condition, with a 32% reduction in TEER loss at 90 min ($P < 0.01$;
186 Fig. 4a). FD4 permeation was also reduced in the GSPE-DSS conditions by 66-73% ($P < 0.05$; Fig.
187 4b). We did not find any significant effect of the preventive GSPE treatments on TEER or FD4
188 permeation in the distal colon.

189 *Basal release of pro-inflammatory cytokines*

190 We found detectable concentrations of the proinflammatory cytokines TNF- α and IL-1 β in
191 the basolateral media of the Ussing chamber at 90 min of incubation. While similar basal levels
192 of TNF- α were found in the proximal and distal colon ($P > 0.05$; Fig. 4a), the basal release of IL-1 β
193 was approximately 3-fold higher in the latter ($P < 0.05$; Fig. 5b).

194 *A preventive GSPE treatment reduces DSS-induced TNF- α release in the proximal colon and modulates*
195 *IL-1 β release in the distal colon.*

196 DSS increased (61%) TNF- α release in the proximal colon at 90 min ($P<0.01$; Fig. 5a);
197 however, we did not observe significant changes in the distal colon (Fig. 5b). In addition, DSS did
198 not change IL-1 β release significantly in the proximal or distal colon. Lastly, the preventive GSPE
199 treatment reduced the DSS-induced TNF- α release of the proximal colon by 22-33% (Fig. 5a),
200 although only GSPE200-DSS exerted a significant effect ($P<0.05$). We did not find any significant
201 effect of GSPE on the TNF- α release of the distal colon; however, GSPE200-DSS modulated IL-1 β
202 secretion in this tissue with a 56% reduction with respect to the control ($P<0.05$; Fig. 5b).

203 **4. Discussion**

204 We developed a feasible ex vivo Ussing chamber-based model to analyze the therapeutic
205 potential of GSPE in human colon tissues exposed to a detrimental chemical agent (DSS), thus
206 avoiding some of the challenges and limitations of in vivo studies in humans [22].

207 In our model, TEER of the control conditions of both proximal and distal colon tissues was
208 very stable during the Ussing chamber experiments. In previous studies, TEER values of 29-39
209 ohm cm² have been found in distal colon tissues taken from endoscopy biopsies [23] and
210 approximately 109-120 ohm cm² in tissues from different colonic locations obtained from surgical
211 procedures [20, 24]. Basal electrophysiological parameters usually vary greatly even within
212 segments of the same tissue. This variability has been described in other ex vivo studies
213 performed with the human intestine [25]; however, regional variations in colonic integrity have
214 not been studied extensively. It is noteworthy that we observed a higher TEER and lower
215 macromolecular permeation in the proximal colon compared to the distal colon, which suggests
216 a decline in tissue integrity along the large intestine. These findings replicate regional variations
217 of colonic integrity observed in rats [26, 27] and are in agreement with results obtained in a recent
218 study performed with colon biopsies of healthy donors [27].

219 The effect of DSS on TEER was particularly severe in the proximal colon and consistent with
220 the enhanced macromolecular permeability also found in this tissue. Our results are in agreement
221 with in vitro studies performed in human epithelial colorectal adenocarcinoma Caco-2 cells,
222 where DSS added apically rapidly decreased monolayer TEER [28, 29] and led to an enhanced
223 FD4 permeation to the basolateral medium [29, 30]. These similarities validate our ex vivo model
224 with the added value of preserving the tissue architecture and cell diversity, features not achieved
225 with in vitro models.

226 We also examined the immune system response to DSS to get a more in-depth
227 characterization of the ex vivo model. The activation of the intestinal immune system due to the
228 epithelial barrier alterations leads to the production of inflammatory mediators [31, 32]. Our
229 results show that the detrimental stimuli of DSS produces slight but significant increases in
230 TNF- α release in the proximal colon after a short period of time. TNF- α is a key
231 immunoregulatory cytokine mainly secreted by the monocytic lineage that amplifies the
232 inflammatory response to recruit other immune cells [33]. Histochemical analyses of uptake and
233 tissue distribution of DSS in mice indicate that DSS rapidly penetrates the colon mucosa and small
234 amounts are found in resident macrophages as early as the day after administration [34]. Since
235 most of the resident macrophages of the lamina propria are hypo-responsive to proinflammatory
236 elements as an adaptation to the antigen-rich microenvironment [35], the DSS-induced release of
237 TNF- α seen here probably reflects the small number of CD14⁺ macrophages of normal mucosa
238 that are involved in sensing bacterial LPS [36]. It cannot be ruled out that other cell types
239 contribute to this because intestinal epithelial cells may also secrete TNF- α in an injury context
240 [37].

241 Once a robust human ex vivo model of intestinal dysfunction had been defined, we assessed
242 the potential gut-protective effects of grape-seed proanthocyanidins. Incubation with the GSPE
243 prior to the DSS treatment attenuated the integrity loss and the concomitant increase in

244 macromolecular permeation induced by DSS in the proximal colon. Indeed, both dietary and
245 pharmacological doses of GSPE administered sub-chronically in rats prevented intestinal
246 permeation after intraperitoneal injection of LPS [38]. In addition, we have previously reported
247 the upregulation of genes involved in the reinforcement of tight-junction (TJ) in the intestine of
248 diet-induced obese rats by dietary and pharmacological GSPE doses with different frequencies of
249 oral administration [11, 39, 40]. The effect of proanthocyanidins on the TJ protein gene expression
250 was recently described in LPS-induced Caco-2 cells co-treated with a procyanidin-rich apple
251 extract [41].

252 The GSPE ($200 \mu\text{g mL}^{-1}$) also attenuated the increase in TNF- α release induced by DSS in the
253 proximal colon. This effect is in line with (1) the reduction of macromolecular permeation across
254 the mucosa and (2) the anti-inflammatory action of the GSPE suppressing the NF- κB
255 inflammatory signal pathway described elsewhere [17, 18, 42]. Remarkably, the barrier protective
256 and anti-inflammatory effects of GSPE in the proximal colon were long-lasting because they were
257 still exhibited after the media were washed out completely. Thus, beneficial long-lasting effects
258 of a sub-chronic oral GSPE treatment on cafeteria diet-induced alterations (including intestinal
259 inflammation) have been described in rats, but the associated mechanisms need to be studied
260 further [11, 43]. The reduction of IL-1 β release estimated in the distal colon is also notable as this
261 cytokine appears to be key in the onset of diarrhea, the main symptom of severe intestinal
262 inflammation [44].

263 Finally, some considerations should be taken into account. First, the colorectal tumor is not
264 an isolated entity but rather may alter both the macromolecular permeability [26] and the gene
265 expression of non-tumor adjacent mucosa [45]. Thus, although colon segments used in this work
266 were anatomopathologically tested, it cannot be ruled out that the integrity and metabolism of
267 healthy tissues could be influenced by their proximity to cancerous lesions. **Second,**
268 **proanthocyanidins are partially degraded in vivo in low molecular weight phenolics by the**

269 intestinal microbiota, thus altering the bioavailability and bioactivity of the parent compounds
270 [46, 47]. Some microbial products of proanthocyanidin degradation exhibit anti-inflammatory
271 properties and likely account for part of the beneficial effects associated with proanthocyanidin
272 consumption in the intestinal mucosa and a large proportion of their effects at systemic level [48].
273 Here we exposed human colon tissues to the parent compounds of the GSPE for a short time
274 window, which is feasible in vivo in the proximal colon [49, 50]. However, the presence of these
275 compounds is less likely in distal regions. In this scenario, it is also important to take into
276 consideration the presence of intestinal microbiota in our samples, which can metabolize the
277 GSPE. In this study the preparation of the biological samples did not undergo a thorough
278 cleansing to avoid undesirable changes in the integrity of tissues. Then, in our ex vivo model, the
279 presence of remnants of microbiota was likely and some degree of microbial degradation of the
280 parent compounds would be expected. Third, it is very difficult to translate the concentrations
281 tested here (50-200 $\mu\text{g mL}^{-1}$) into oral doses intended for therapy; however, the gut-protective
282 effects of GSPE found in this work would probably only be achieved in humans with
283 pharmacological doses. A recent study conducted in healthy humans found that the daily
284 ingestion of oral pharmacological doses of GSPE (1000-2500 mg) in healthy adults is safe and
285 doses are well tolerated during a 4-week period [51]. Therefore, effective GSPE doses in humans
286 need to be established by further clinical trials.

287 Taken together, our results indicate that the detrimental effect of DSS on tissue integrity,
288 extent of paracellular pathway opening and local inflammatory response were more prominent
289 in the proximal colon. We found that GSPE administered as a treatment prior to damage
290 induction dose-dependently attenuated the epithelial barrier disruption and the local
291 inflammatory response of the proximal colon. Furthermore, these effects were long-lasting and
292 endured even though proanthocyanidins were not present. The distal colon was not responsive
293 to the preventive treatment; however, basal IL-1 β release decreased with high concentrations of
294 GSPE. Therefore, our results demonstrate the potential preventive effects of GSPE on the acute

295 dysfunction of the human colon. Controlled trials are necessary to test the administration of GSPE
296 as a complementary therapeutic approach for the colonic dysfunction associated with metabolic
297 disorders and IBD.

298 **5. Acknowledgments**

299 This research was funded by the Spanish Ministerio de Economía y Competitividad, grants
300 AGL2014-55347-R, AGL2017-83477-R, and 2014LINE-06 grant from the URV-Banco Santander. C.
301 González-Quilen received financial support through a FI-AGAUR grant from the Generalitat de
302 Catalunya, C. Grau-Bové is student fellow in the Martí i Franquès program of the Universitat
303 Rovira i Virgili, Tarragona, Spain. M. Pinent and X. Terra are Serra-Húnter fellows at the
304 Universitat Rovira i Virgili, Tarragona, Spain.

305 The authors declare that they have no conflict of interest.

6. References

- 306
- 307 1. Chelakkot C, Ghim J, Ryu SH (2018) Mechanisms regulating intestinal barrier integrity
308 and its pathological implications. *Exp. Mol. Med.* 50:103
- 309 2. Hamilton MK, Boudry G, Lemay DG, Raybould HE (2015) Changes in intestinal barrier
310 function and gut microbiota in high-fat diet-fed rats are dynamic and region dependent.
311 *Am J Physiol Gastrointest Liver Physiol* 308:G840-51.
312 <https://doi.org/10.1152/ajpgi.00029.2015>
- 313 3. Neurath MF (2014) Cytokines in inflammatory bowel disease. *Nat Rev Immunol* 14:329–
314 342. <https://doi.org/10.1038/nri3661>
- 315 4. Duan Y, Zeng L, Zheng C, et al (2018) Inflammatory links between high fat diets and
316 diseases. *Front Immunol* 9:2649. <https://doi.org/10.3389/fimmu.2018.02649>
- 317 5. Boutagy NE, McMillan RP, Frisard MI, Hulver MW (2016) Metabolic endotoxemia with
318 obesity: Is it real and is it relevant? *Biochimie* 124:11–20.
319 <https://doi.org/10.1016/j.biochi.2015.06.020>
- 320 6. Fukui H (2016) Increased Intestinal Permeability and Decreased Barrier Function: Does It
321 Really Influence the Risk of Inflammation? *Inflamm Intest Dis* 1:135–145.
322 <https://doi.org/10.1159/000447252>
- 323 7. Randhawa PK, Singh K, Singh N, Jaggi AS (2014) A review on chemical-induced
324 inflammatory bowel disease models in rodents. *Korean J Physiol Pharmacol* 18:279–88.
325 <https://doi.org/10.4196/kjpp.2014.18.4.279>
- 326 8. Eichele DD, Kharbanda KK (2017) Dextran sodium sulfate colitis murine model: An
327 indispensable tool for advancing our understanding of inflammatory bowel diseases
328 pathogenesis. *World J Gastroenterol* 23:6016–6029.
329 <https://doi.org/10.3748/wjg.v23.i33.6016>

- 330 9. Laroui H, Ingersoll SA, Liu HC, et al (2012) Dextran sodium sulfate (DSS) induces colitis
331 in mice by forming nano-lipocomplexes with medium-chain-length fatty acids in the
332 colon. *PLoS One* 7:e32084. <https://doi.org/10.1371/journal.pone.0032084>
- 333 10. Masumoto S, Terao A, Yamamoto Y, et al (2016) Non-absorbable apple procyanidins
334 prevent obesity associated with gut microbial and metabolomic changes. *Sci Rep*
335 6:31208. <https://doi.org/10.1038/srep31208>
- 336 11. Gil-Cardoso K, Ginés I, Pinent M, et al (2018) The co-administration of
337 proanthocyanidins and an obesogenic diet prevents the increase in intestinal
338 permeability and metabolic endotoxemia derived to the diet. *J Nutr Biochem* 62:35–42.
339 <https://doi.org/10.1016/j.jnutbio.2018.07.012>
- 340 12. Martin DA, Bolling BW (2015) A review of the efficacy of dietary polyphenols in
341 experimental models of inflammatory bowel diseases. *Food Funct* 6:1773–86.
342 <https://doi.org/10.1039/c5fo00202h>
- 343 13. Smeriglio A, Barreca D, Bellocco E, Trombetta D (2017) Proanthocyanidins and
344 hydrolysable tannins: occurrence, dietary intake and pharmacological effects. *Br J*
345 *Pharmacol* 174:1244–1262. <https://doi.org/10.1111/bph.13630>
- 346 14. Li X-L, Cai Y-Q, Qin H, Wu Y-J (2008) Therapeutic effect and mechanism of
347 proanthocyanidins from grape seeds in rats with TNBS-induced ulcerative colitis. *Can J*
348 *Physiol Pharmacol* 86:841–849. <https://doi.org/10.1139/Y08-089>
- 349 15. Wang Y-H, Yang X-L, Wang L, et al (2010) Effects of proanthocyanidins from grape seed
350 on treatment of recurrent ulcerative colitis in rats. *Can J Physiol Pharmacol* 88:888–898.
351 <https://doi.org/10.1139/Y10-071>
- 352 16. Cheah KY, Bastian SEP, Acott TM V., et al (2013) Grape Seed Extract Reduces the
353 Severity of Selected Disease Markers in the Proximal Colon of Dextran Sulphate Sodium-

- 354 Induced Colitis in Rats. *Dig Dis Sci* 58:970–977. <https://doi.org/10.1007/s10620-012-2464-1>
- 355 17. Terra X, Valls J, Vitrac X, et al (2007) Grape-seed procyanidins act as antiinflammatory
356 agents in endotoxin-stimulated RAW 264.7 macrophages by inhibiting NFκB signaling
357 pathway. *J Agric Food Chem* 55:4357–4365. <https://doi.org/10.1021/jf0633185>
- 358 18. Wang Y-H, Ge B, Yang X-L, et al (2011) Proanthocyanidins from grape seeds modulates
359 the nuclear factor-kappa B signal transduction pathways in rats with TNBS-induced
360 recurrent ulcerative colitis. *Int Immunopharmacol* 11:1620–1627.
361 <https://doi.org/10.1016/j.intimp.2011.05.024>
- 362 19. Geraedts MCP, Troost FJ, Tinnemans R, et al (2010) Release of satiety hormones in
363 response to specific dietary proteins is different between human and murine small
364 intestinal mucosa. *Ann Nutr Metab* 56:308–313. <https://doi.org/10.1159/000312664>
- 365 20. Sjöberg Å, Lutz M, Tannergren C, et al (2013) Comprehensive study on regional human
366 intestinal permeability and prediction of fraction absorbed of drugs using the Ussing
367 chamber technique. *Eur J Pharm Sci* 48:166–180.
368 <https://doi.org/10.1016/J.EJPS.2012.10.007>
- 369 21. Margalef M, Pons Z, Iglesias-Carres L, et al (2016) Gender-related similarities and
370 differences in the body distribution of grape seed flavanols in rats. *Mol Nutr Food Res*
371 60:760–772. <https://doi.org/10.1002/mnfr.201500717>
- 372 22. Pizarro TT, Stappenbeck TS, Rieder F, et al (2019) Challenges in IBD Research: Preclinical
373 Human IBD Mechanisms. *Inflamm Bowel Dis* 25:S5–S12.
374 <https://doi.org/10.1093/ibd/izz075>
- 375 23. Wallon C, Braaf Y, Wolving M, et al (2005) Endoscopic biopsies in Ussing chambers
376 evaluated for studies of macromolecular permeability in the human colon. *Scand J*
377 *Gastroenterol* 40:586–595. <https://doi.org/10.1080/00365520510012235>

- 378 24. Schmitz H, Barmeyer C, Gitter AH, et al (2006) Epithelial Barrier and Transport Function
379 of the Colon in Ulcerative Colitis. *Ann N Y Acad Sci* 915:312–326.
380 <https://doi.org/10.1111/j.1749-6632.2000.tb05259.x>
- 381 25. Geraedts MCP, Troost FJ, De Ridder RJ, et al (2012) Validation of Ussing chamber
382 technology to study satiety hormone release from human duodenal specimens. *Obesity*
383 20:678–682. <https://doi.org/10.1038/oby.2011.104>
- 384 26. Viktoria VB, Evgeny LF, Larisa SO, et al (2018) Increased paracellular permeability of
385 tumor-adjacent areas in 1,2-dimethylhydrazine-induced colon carcinogenesis in rats.
386 *Cancer Biol Med* 15:251. <https://doi.org/10.20892/j.issn.2095-3941.2018.0016>
- 387 27. Thomson A, Smart K, Somerville MS, et al (2019) The Ussing chamber system for
388 measuring intestinal permeability in health and disease. *BMC Gastroenterol* 19:98.
389 <https://doi.org/10.1186/s12876-019-1002-4>
- 390 28. Araki Y, Sugihara H, Hattori T (2006) In vitro effects of dextran sulfate sodium on a
391 Caco-2 cell line and plausible mechanisms for dextran sulfate sodium-induced colitis.
392 *Oncol Rep* 16:1357–62
- 393 29. Zhao H, Zhang H, Wu H, et al (2012) Protective role of 1,25(OH)₂ vitamin D₃ in the
394 mucosal injury and epithelial barrier disruption in DSS-induced acute colitis in mice.
395 *BMC Gastroenterol* 12:57. <https://doi.org/10.1186/1471-230X-12-57>
- 396 30. Zhao H, Yan R, Zhou X, et al (2016) Hydrogen sulfide improves colonic barrier integrity
397 in DSS-induced inflammation in Caco-2 cells and mice. *Int Immunopharmacol* 39:121–
398 127. <https://doi.org/10.1016/j.intimp.2016.07.020>
- 399 31. Van Dijk APM, Keuskamp ZJ, Wilson JHP, Zijlstra FJ (1995) Sequential release of
400 cytokines, lipid mediators and nitric oxide in experimental colitis. *Mediators Inflamm*
401 4:186–190. <https://doi.org/10.1155/S0962935195000305>

- 402 32. Nagib MM, Tadros MG, Elsayed MI, Khalifa AE (2013) Anti-inflammatory and anti-
403 oxidant activities of olmesartan medoxomil ameliorate experimental colitis in rats.
404 *Toxicol Appl Pharmacol* 271:106–113. <https://doi.org/10.1016/j.taap.2013.04.026>
- 405 33. Ruder B, Atreya R, Becker C (2019) Tumour Necrosis Factor Alpha in Intestinal
406 Homeostasis and Gut Related Diseases. *Int J Mol Sci* 20:.
407 <https://doi.org/10.3390/ijms20081887>
- 408 34. Kitajima S, Takuma S, Morimoto M (1999) Tissue distribution of dextran sulfate sodium
409 (DSS) in the acute phase of murine DSS-induced colitis. *J Vet Med Sci* 61:67–70.
410 <https://doi.org/10.1292/jvms.61.67>
- 411 35. Smythies LE, Sellers M, Clements RH, et al (2005) Human intestinal macrophages
412 display profound inflammatory anergy despite avid phagocytic and bacteriocidal
413 activity. *J Clin Invest* 115:66. <https://doi.org/10.1172/JCI19229>
- 414 36. Kamada N, Hisamatsu T, Okamoto S, et al (2008) Unique CD14 intestinal macrophages
415 contribute to the pathogenesis of Crohn disease via IL-23/IFN-gamma axis. *J Clin Invest*
416 118:2269–80. <https://doi.org/10.1172/JCI34610>
- 417 37. Roulis M, Armaka M, Manoloukos M, et al (2011) Intestinal epithelial cells as producers
418 but not targets of chronic TNF suffice to cause murine Crohn-like pathology. *Proc Natl*
419 *Acad Sci U S A* 108:5396–401. <https://doi.org/10.1073/pnas.1007811108>
- 420 38. Gil-Cardoso K, Comitato R, Ginés I, et al (2019) Protective Effect of Proanthocyanidins in
421 a Rat Model of Mild Intestinal Inflammation and Impaired Intestinal Permeability
422 Induced by LPS. *Mol Nutr Food Res* 63:1800720. <https://doi.org/10.1002/mnfr.201800720>
- 423 39. Gil-Cardoso K, Ginés I, Pinent M, et al (2017) Chronic supplementation with dietary
424 proanthocyanidins protects from diet-induced intestinal alterations in obese rats. *Mol*
425 *Nutr Food Res* 61:1601039. <https://doi.org/10.1002/mnfr.201601039>

- 426 40. González-Quilen C, Gil-Cardoso K, Ginés I, et al (2019) Grape-seed proanthocyanidins
427 are able to reverse intestinal dysfunction and metabolic endotoxemia induced by a
428 cafeteria diet in wistar rats. *Nutrients* 11:. <https://doi.org/10.3390/nu11050979>
- 429 41. Wu H, Luo T, Li YM, et al (2018) Granny Smith apple procyanidin extract upregulates
430 tight junction protein expression and modulates oxidative stress and inflammation in
431 lipopolysaccharide-induced Caco-2 cells. *Food Funct* 9:3321–3329.
432 <https://doi.org/10.1039/c8fo00525g>
- 433 42. Li X, Yang X, Cai Y, et al (2011) Proanthocyanidins from Grape Seeds Modulate the NF-
434 κ B Signal Transduction Pathways in Rats with TNBS-Induced Ulcerative Colitis.
435 *Molecules* 16:6721–6731. <https://doi.org/10.3390/molecules16086721>
- 436 43. Ginés I, Gil-Cardoso K, Serrano J, et al (2018) Effects of an Intermittent Grape-Seed
437 Proanthocyanidin (GSPE) Treatment on a Cafeteria Diet Obesogenic Challenge in Rats.
438 *Nutrients* 10:315. <https://doi.org/10.3390/nu10030315>
- 439 44. Siegmund B, Lehr H-A, Fantuzzi G, Dinarello CA (2001) IL-1 -converting enzyme
440 (caspase-1) in intestinal inflammation. *Proc Natl Acad Sci* 98:13249–13254.
441 <https://doi.org/10.1073/pnas.231473998>
- 442 45. Sanz-Pamplona R, Berenguer A, Cordero D, et al (2014) Aberrant gene expression in
443 mucosa adjacent to tumor reveals a molecular crosstalk in colon cancer. *Mol Cancer*
444 13:46. <https://doi.org/10.1186/1476-4598-13-46>
- 445 46. Monagas M, Urpi-Sarda M, Sánchez-Patán F, et al (2010) Insights into the metabolism
446 and microbial biotransformation of dietary flavan-3-ols and the bioactivity of their
447 metabolites. *Food Funct*. 1:233–253
- 448 47. Margalef M, Pons Z, Bravo FI, et al (2015) Plasma kinetics and microbial
449 biotransformation of grape seed flavanols in rats. *J Funct Foods* 12:478–488.

- 450 <https://doi.org/10.1016/j.jff.2014.12.007>
- 451 48. Mena P, Bresciani L, Brindani N, et al (2019) Phenyl- γ -valerolactones and phenylvaleric
452 acids, the main colonic metabolites of flavan-3-ols: Synthesis, analysis, bioavailability,
453 and bioactivity. *Nat. Prod. Rep.* 36:714–752
- 454 49. Wiese S, Esatbeyoglu T, Winterhalter P, et al (2015) Comparative biokinetics and
455 metabolism of pure monomeric, dimeric, and polymeric flavan-3-ols: A randomized
456 cross-over study in humans. *Mol Nutr Food Res* 59:610–621.
457 <https://doi.org/10.1002/mnfr.201400422>
- 458 50. Castello F, Costabile G, Bresciani L, et al (2018) Bioavailability and pharmacokinetic
459 profile of grape pomace phenolic compounds in humans. *Arch Biochem Biophys* 646:1–
460 9. <https://doi.org/10.1016/j.abb.2018.03.021>
- 461 51. Sano A (2017) Safety assessment of 4-week oral intake of proanthocyanidin-rich grape
462 seed extract in healthy subjects. *Food Chem Toxicol* 108:519–523.
463 <https://doi.org/10.1016/j.fct.2016.11.021>

464

465 **7. Figure captions.**

466 **Fig. 1** Schematic diagram of the experimental protocol. For each experiment carried out, four
467 stripped proximal or distal colon segments of one patient were randomly assigned to one of four
468 experimental conditions. Ctrl (control), only Krebs-Ringer bicarbonate (KRB) buffer; DSS, acute
469 colonic dysfunction induced by 12% of dextran sodium sulphate in KRB buffer; GSPE-DSS,
470 incubation with the grape-seed proanthocyanidin extract (GSPE) followed by DSS-induced acute
471 colonic dysfunction. Specified media were added apically. KRB-glucose buffer with protease
472 inhibitors was used in the basolateral compartment (see text for details).

473 **Fig. 2** Haematoxylin-eosin staining of transversal sections from the human colon before (a) and
474 after (b) the serosal and outer muscular layers were removed. The muscularis externa is
475 completely absent after stripping.

476 **Fig. 3** Linear relationships between age, BMI and TEER values in the proximal (a) and distal (b)
477 colon. The inset shows the Pearson's r correlation and the corresponding P-value

478 **Fig. 4** Effect of the preventive GSPE treatment on TEER (a) and FD4 relative permeation (b) in
479 DSS-induced dysfunctional human colon. GSPE (50 and 200 $\mu\text{g mL}^{-1}$) was incubated apically
480 during the first 30 min at 37 °C. After a washout, DSS at 12% was added apically (black arrows)
481 and maintained until the end of the experiment. Ctrl (control), only Krebs-Ringer bicarbonate
482 buffer. FD4 was added apically at 30 min and determined from the basolateral media at 90 min.
483 The dashed lines indicate the basal FD4 permeation (Ctrl condition). Values are presented as
484 mean \pm SEM. The sample size for each variable was: TEER (proximal, distal colon), Ctrl $n=26$,
485 $n=21$; DSS $n=27$, $n=23$; GSPE50-DSS $n=23$, $n=19$; GSPE200-DSS $n=22$, $n=17$. FD4 permeation
486 (proximal, distal colon), Ctrl $n=15$, $n=14$; DSS $n=15$, $n=13$; GSPE50-DSS $n=13$, $n=7$; GSPE200-DSS
487 $n=10$, $n=10$. * $P<0.05$ versus control; # $P<0.05$ versus DSS.

488 **Fig. 5** Effect of the preventive GSPE treatment on the secretion levels of TNF- α (a) and IL-1 β (b)
489 in DSS-induced dysfunctional human colon. Ctrl (control), only Krebs-Ringer bicarbonate (KRB)
490 buffer; DSS, acute dysfunction induced by 12% of dextran sodium sulphate in KRB buffer; GSPE-
491 DSS, incubation with the GSPE followed by DSS-induced acute dysfunction. Values are presented
492 as mean \pm SEM. The sample size for each variable was: TNF- α (proximal, distal colon), Ctrl $n=20$,
493 $n=19$; DSS $n=20$, $n=19$; GSPE50-DSS $n=17$, $n=15$; GSPE200-DSS $n=16$, $n=14$. IL-1 β (proximal, distal
494 colon), Ctrl $n=14$, $n=19$; DSS $n=14$, $n=19$; GSPE50-DSS $n=12$, $n=14$; GSPE200-DSS $n=12$, $n=14$.
495 * $P<0.05$ versus control; # $P<0.05$ versus DSS.

Figure 2

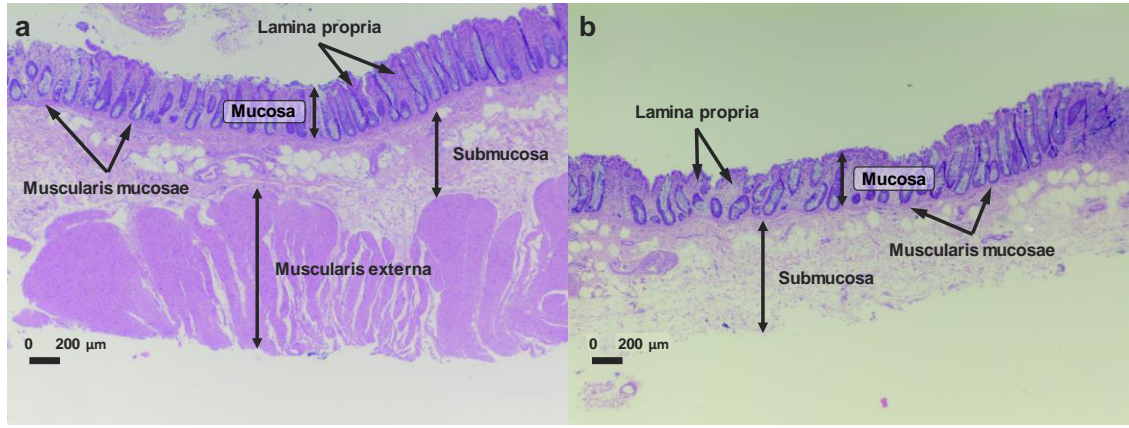


Figure 3

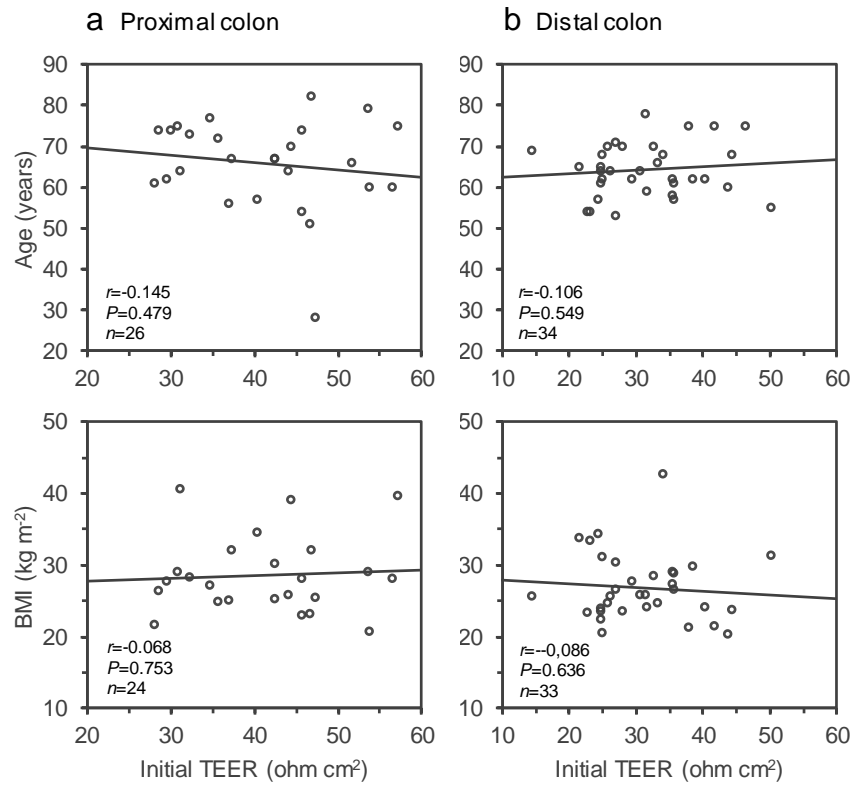


Figure 5

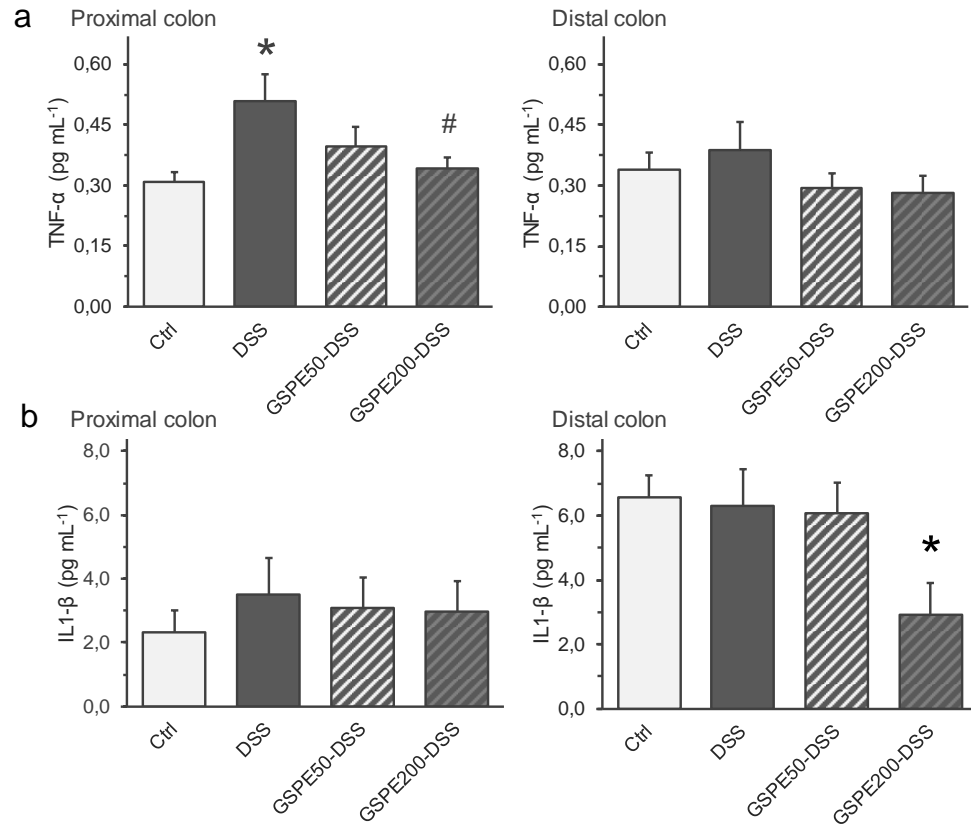


Figure 4

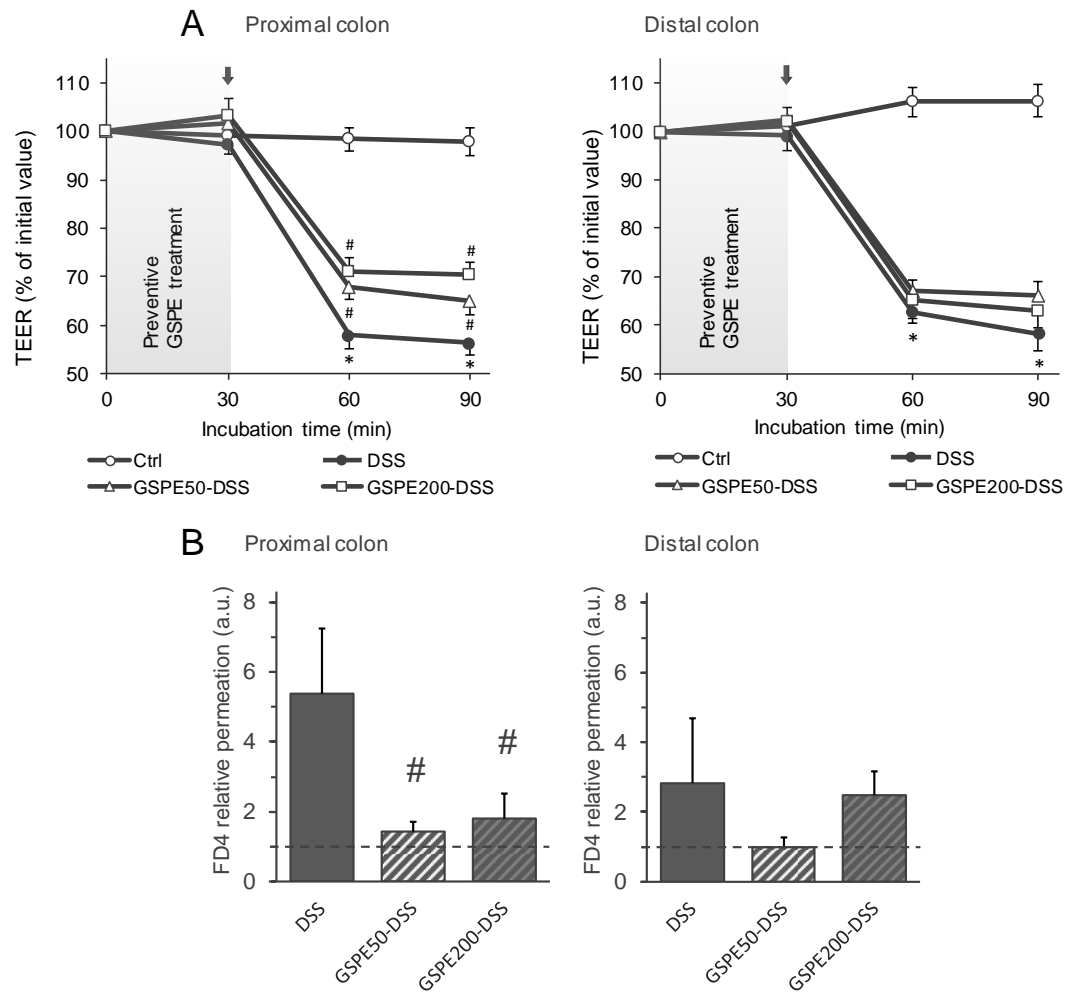


Figure 1

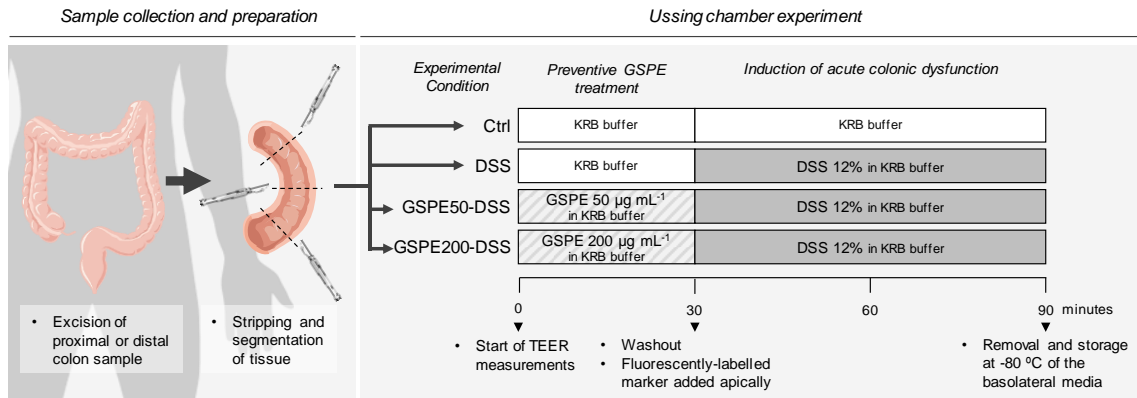


Table 1. Descriptive statistic and biochemical parameters of the donor patients.

	All (n=61)	Proximal colon donors (n=27)	Distal colon donors (n=34)
Age (years)			
<50	14 (22.5%)	5 (18.5%)	9 (25.7%)
50-60	30 (48.4%)	12 (44.5%)	18 (51.4%)
>60	18 (29.0%)	10 (37.0%)	8 (22.9%)
Gender			
Male	34 (54.8%)	13 (48.1%)	21 (60.0%)
Female	28 (45.2%)	14 (51.9%)	14 (40.0%)
Tobacco consumption			
Never	50 (80.6%)	20 (74.0%)	30 (85.7%)
<20 cigarettes per day	9 (14.5%)	4 (14.8%)	5 (14.3%)
>20 cigarettes per day	3 (4.9%)	3 (11.2%)	0 (0.0%)
Alcohol consumption			
Never	35 (56.4%)	14 (52.4%)	20 (58.1%)
Mild-Moderate	27 (43.6%)	13 (47.6%)	15 (41.9%)
BMI (kg m⁻²)	27.6 ± 0.7	28.1 ± 1.1	27.3 ± 0.8
Glucose (mM)	5.8 ± 0.2	5.7 ± 0.4	5.9 ± 0.3
Cholesterol (mg dL⁻¹)			
Total	187.4 ± 5.6	183.0 ± 9.6	190.0 ± 6.9
HDL	55.4 ± 3.7	53.0 ± 6.5	57.0 ± 4.3
LDL	108.1 ± 7.8	100.8 ± 10.3	114.1 ± 11.4
Triglycerides (mg dL⁻¹)	114.2 ± 7.7	105.3 ± 10.2	120.0 ± 10.1

Data is presented as number of patients (percentage) or mean ± SEM.